Title

GEOMETRIC DESIGN OF A PASSIVE MECHANICAL KNEE FOR LOWER EXTREMITY WEARABLE DEVICES BASED ON ANTHROPOMORPHIC FOOT TASK GEOMETRY SCALING

ISBN

978-0-7918-5713-7

Authors

Ghosh, Shramana
Robson, Nina
McCarthy, JM

Publication Date

2016

DOI

10.1115/DETC201546499

Peer reviewed

Proceedings of the ASME 2015 International Design Engineering Technical Conferences & Computers and Information in Engineering Conference
IDETC/CIE 2015
August 2-5, 2015, Boston, Massachusetts, USA

DETC2015-46499

GEOMETRIC DESIGN OF A PASSIVE MECHANICAL KNEE FOR LOWER EXTREMITY WEARABLE DEVICES BASED ON ANTHROPOMORPHIC FOOT TASK GEOMETRY SCALING

Shramana Ghosh *
Mechanical and Aerospace Engineering
University of California
Irvine, California 92697
Email: shramang@uci.edu

Nina Robson
Mechanical Engineering
California State University
Fullerton, California 92834
Mechanical and Aerospace Engineering
University of California
Irvine, California 92697
Email: nrobson@fullerton.edu

J. M. McCarthy
Mechanical and Aerospace Engineering
University of California
Irvine, California 92697
Email: jmmccart@uci.edu

ABSTRACT

The standard recovery treatment for ankle and lower leg injuries consists of using underarm crutches. Hands-free crutches have recently emerged as a more comfortable, natural and energy efficient alternative. However in the currently available devices such as the iWalk-Free (iWALKFree, Inc., USA) the lack of a knee joint results in abnormal motion pattern at the hip and pelvic joints to ensure foot clearance during the swing phase of the gait. To address this shortcoming, the paper describes the kinematic synthesis of a planar passive four-bar linkage that can be used as a mechanical knee in lower limb exoskeletons and other wearable devices. The knee design is based on anthropomorphic foot walking trajectory obtained from optical motion capture system. The task geometry at the foot, related to the contact and curvature constraints between the foot and the ground at two critical positions 'heel strike' and 'toe off' is scaled to the knee level. Velocity and acceleration specifications compatible with the contact and curvature constraints assist in defining the synthesis equations for the knee design. A working prototype of a passive wearable crutch substitute that incorporates the mechanical knee shows the applicability of the proposed technique.

*Address all correspondence to this author.

INTRODUCTION

Currently existing knee joint mechanisms can be classified as knee joints with either single axis of rotation or multiple axes of rotation [1]. Knees with a single revolute joint fall under the category of single-axis knees, and cannot simulate natural human motion well. Knee joints with variable instantaneous center of rotation (also called multi-axis knees) are composed of multi-bar mechanisms, most commonly the four-bar mechanism.

Human knee can be modeled as a planar single degree of freedom four-bar linkage. This model is a key tool for designing reliable and efficient prosthetic devices [2]. Radcliffe [3] described the kinematic characteristics and advantages of four-bar linkage based knee mechanisms. An analysis of the strengths and weaknesses of four-bar linkage knee mechanisms for clinicians prescribing prosthetics was given by de Vries [4]. More recently, Sancisi, Caminati and Parenti-Castelli [5], Xie, Lian, Li and Guo [1], Hamon and Aoustin [6] and Jin, Zhang, Dimo, Wang and Zhang [7] have reported designs of knee joints using multi-bar mechanisms. Multi-axis knee joints can be made to have greater security and reliability by moving the instantaneous center of the mechanism lower and backward, compared to single-axis knees by the addition of extra links. Sancisi, Caminati and Parenti-Castelli [5] describe a modified optimization procedure for synthesis of a four-bar mechanism that has motion

similar to experimentally observed motion and satisfies requirements on centrode to ensure stability of the prosthesis. Hamon and Aoustin [6] propose a design of a cross four-bar linkage that has optimal energetic trajectory. Jin, Zhang, Dimo, Wang and Zhang [7] design a six-bar linkage for the knee joint based on optimization procedure to find designs that met the requirements imposed on the location of the geometric center of the mechanism and to ensure stability in the extended position of the knee.

This paper reports the application of a recent planar contact synthesis technique, developed by Robson and McCarthy [8], to the design of a passive mechanical knee. Objects in the environment impose velocity and acceleration specifications related to contact and curvature constraints on the movement of the foot. These constraints are linearly scaled to the knee level and have to be satisfied by the chain to be synthesized. The synthesis of planar linkages for velocity and acceleration constraints was formulated by Tesar [9] and Dowler, Duffy and Tesar [10]. The concept of using relative curvature of surfaces in contact to limit the movement of a workpiece was introduced by Rimon and Burdick [11] and [12]. They generalized the study of the grasping constraint of a rigid body using the fingers of a mechanical hand by considering the configuration space of movement of the body relative to obstacles formed by the fingers, and introduced the idea of second order mobility of a constrained body. Subsequently, Robson and McCarthy [8] used this viewpoint to develop a synthesis technique that can guide an end-effector/floating link such that it satisfies contact constraints. They show how to use the relative curvature of the contact of the end-effector with one or more objects to define velocity and acceleration specifications for its movement. The obtained kinematic constraints can be used to synthesize the dimensions of the serial chain.

The contribution of this paper is in designing a passive four-bar linkage knee, based on contact and curvature constraints, derived from the anthropomorphic foot trajectory in the vicinity of two critical positions. This paper demonstrates the application of these results, showing how higher order motion constraints and their scaling can be used in the synthesis of a four-bar knee with the main design goals of simple and compact structure, as well as ability to mimic the natural human walking gait.

PLANAR CONTACT DIRECTION AND CURVATURE

Let the movement of a rigid body AB (shown in Figure 1) be defined by the 3×3 homogeneous transforms $[T(t)] = [R(t), \mathbf{d}(t)]$ constructed from a rotation matrix, $R(t)$, and translation vector $\mathbf{d}(t)$. In the particular case of the foot contacting the ground, A and B represent the locations of the heel and the toe. Any point $\mathbf{p}$ on the foot with an attached moving frame M traces a trajectory $\mathbf{P}(t)$ in a fixed coordinate frame F, given by

$$\mathbf{P(t)} = [T(t)]\mathbf{p} = \begin{bmatrix} \cos\phi(t) & -\sin\phi(t) & d_x(t) \\ \sin\phi(t) & \cos\phi(t) & d_y(t) \\ 0 & 0 & 1 \end{bmatrix} \begin{Bmatrix} p_x \\ p_y \\ 1 \end{Bmatrix} \quad (1)$$

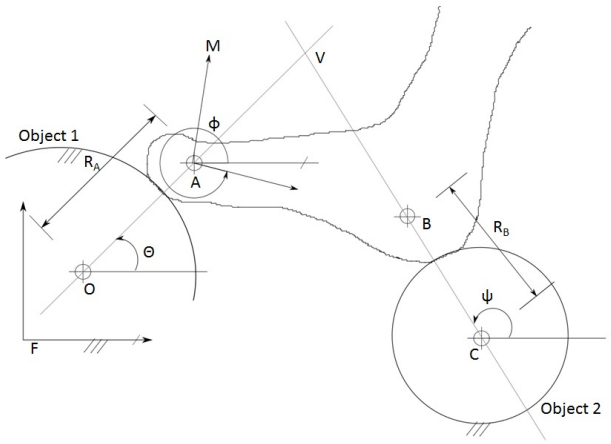

FIGURE 1. The body with attched Frame M moves in contact with two objects such that the trajectories of **A** and **B** have the radii of curvature, R_A and R_B, respectively.

The Position Specification

Assume that the foot AB moves in contact with two fixed objects, the point trajectories $\mathbf{A}(t)$ and $\mathbf{B}(t)$ are constrained to move on circles in the vicinity of a reference position denoted by $t = 0$, as shown Figure 1.

The movement of the body in the vicinity of $t = 0$ can be expressed as the Taylor series expansion,

$$[T(t)] = [T_0] + [T_1]t + \frac{1}{2}[T_2]t^2 + \ldots \quad \text{where} \quad [T_i] = \frac{d^i[T]}{dt^i} \quad (2)$$

$[T_0]$ can be specified using the data provided for the position of the moving frame M that identifies the coordinates of the contact points $\mathbf{A_0} = \mathbf{A}(0)$ and $\mathbf{B_0} = \mathbf{B}(0)$.

The Velocity Specification

The directions of the velocities vectors $\dot{\mathbf{A}}$ and $\dot{\mathbf{B}}$ are set to be perpendicular to the forces $\mathbf{F_A}$ and $\mathbf{F_B}$ by defining the point of intersection $\mathbf{V}$ of the lines of actions of these two forces to be the velocity pole of the movement of M in this position (Figure

1). This allows calculation of the angular velocities $\mathbf{w_{OA}} = \dot{\theta}\vec{k}$ and $\mathbf{w_{CB}} = \dot{\psi}\vec{k}$. The velocity loop equations of the quadrilateral **OABC** are then used to compute the velocity $\dot{\mathbf{B}} = \dot{\mathbf{A}} + \mathbf{w} \times (\mathbf{B} - \mathbf{A})$. The angular velocity $\phi_1 = \dot{\phi}(0)$ and the velocity $\mathbf{d_1} = \dot{\mathbf{A}}(0)$ define the elements of the velocity matrix $[T_1]$.

The Acceleration Specification

As the body M moves in contact with two objects, the points A and B are guided along trajectories with radii of curvature R_A and R_B. We use the acceleration loop equations of the quadrilateral **OABC**, in order to determine the angular accelerations $\mathbf{a_{OA}} = \ddot{\theta}\vec{k}$ and $\mathbf{a_{CB}} = \ddot{\psi}\vec{k}$ for a given value of the angular acceleration $\mathbf{a} = \ddot{\phi}\vec{k}$. This in turn allows us to determine $\ddot{\mathbf{d}} = \ddot{\mathbf{A}}$. The acceleration loop equations are obtained by computing the time derivative of the velocity loop equations. The values $\phi_2 = 0$ and $\mathbf{d_2} = \ddot{\mathbf{A}}(0)$ determine the elements of the acceleration matrix $[T_2]$.

Relative Movement

For convenience of formulating synthesis equations, we introduce the relative transformation $[D(t)] = [T(t)][T_0]^{-1}$ that operates on point coordinates measured in the fixed frame at the instant $t = 0$. Then we get,

$$\begin{aligned}\mathbf{P(t)} =& [T_0 + T_1 t + \frac{1}{2}T_2 t^2 + \cdots][T_0]^{-1}\mathbf{p} \\ =& [I + \Omega t + \frac{1}{2}\Lambda t^2 + \cdots]\mathbf{p} = [D(t)]\mathbf{p} \end{aligned} \quad (3)$$

where

$$[\Omega] = \begin{bmatrix} 0 & -\phi_1 & d_{x1} + d_{y0}\phi_1 \\ \phi_1 & 0 & d_{y1} - d_{x0}\phi_1 \\ 0 & 0 & 0 \end{bmatrix}$$

$$[\Lambda] = \begin{bmatrix} -\phi_1^2 & -\phi_2 & d_{x2} + d_{x0}\phi_1^2 + d_{y0}\phi_2 \\ \phi_2 & -\phi_1^2 & d_{y2} + d_{y0}\phi_1^2 - d_{x0}\phi_2 \\ 0 & 0 & 0 \end{bmatrix}. \quad (4)$$

For more details on deriving the higher order motion task specification related to contact and curvature constraints, see [13].

PRELIMINARY WORK ON THE DESIGN OF PASSIVE CRUTCHES WITH CONTACT TASK SPECIFICATIONS

In the currently available devices such as the iWalk-Free (iWALKFree, Inc., USA) the lack of a knee joint results in abnormal motion pattern at the hip and pelvic joints, resulting in a non-anthropomorphic gait cycle. To address this shortcoming, three passive walking prototypes were developed, two of which with serial and one with parallel kinematic structure. All three designs were based on anthropomorphic walking trajectory from the foot, obtained from a motion capture system. For the two serial linkage prototypes, the leg was synthesized as an RR planar kinematic chain where the first hinge is located at the hip and the other at the knee joint and animated in Mathematica (Figure 2). The synthesis task consisted of two positions with one velocity defined in each position and one acceleration, defined in the first position. Note, that these velocities and accelerations are derived from the end-foot trajectory and are compatible with contact and curvature constraints between the foot and the ground (for more details see [8]). The performance of both devices was tested in

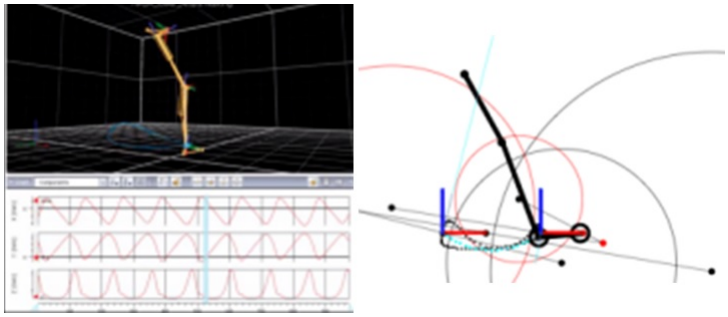

FIGURE 2. Due to the contact and curvature specifications, while leaving the first position the toe and heel of the RR chain emain in contact with two virtual bodies in the vicinity of the two specified positions.

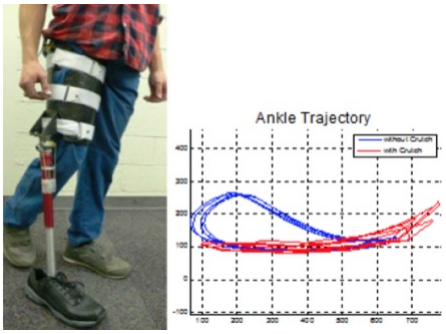

FIGURE 3. Prototype of the first passive walking device developed to assist a person with lower leg injury.

a pilot study with a subject walking on the treadmill operating at a speed of 2 mph. The devices and the end-foot trajectories obtained from them are given in Figure 3 and Figure 4. The design, shown in Figure 4 incorporates an additional sliding joint at the hip level, and demonstrates a better "tear-drop" shape trajectory as traced by the toe. However, this particular design has stability issues. Since both passive devices adopt the single-axis

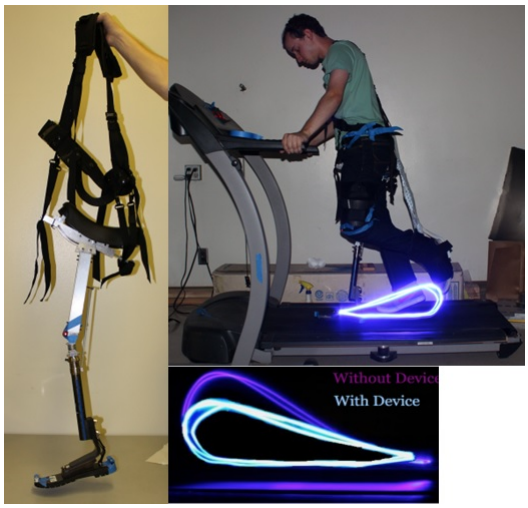

FIGURE 4. Prototype of the second passive walking device developed to assist a person with lower leg injury.

knee joint, which has a fixed center of rotation, they could not simulate human motion very well.

To address that issue, a third wearable passive crutch substitute called TAMC1 with a closed-loop kinematic structure was developed [14]. The crutch is shown in Figure 5 and consists of a five-bar linkage that attaches to the leg and a four bar for the ankle-foot system. The users body weight is supported through a seat located within the thigh region. Although after testing the prototype on a subject volunteer it showed promising results, the device was pretty heavy and bulky. This led us to the idea regarding developing a compact, passive knee design, discussed in the next section.

DESIGN OF THE PASSIVE KNEE MECHANISM BASED ON ANTHROPOMORPHIC END-FOOT TRAJECTORY

To facilitate the design process, a human subject walking on a treadmill was monitored by 3D Motion Capture System as shown in Figure 6. Eight reflective markers were attached on the subjects right leg and the trajectories at the foot, hip and knee joints were obtained (see Figure 7).

Figure 7 presents the heel and knee gait trajectories for one cycle. Note that the geometrical shape of the reference foot trajectory looks like a teardrop for each gait cycle. Sagittal plane walking motion can be assumed as a planar task which consists of positioning the foot, at the point, $Mj(j = 1,\ldots,n)$, located on the reference trajectory. If the kinematic specifications at the start "toe-off" and end "heel-strike" of the walking cycle are acquired, our preliminary data show that it is possible to synthesize a serial RR chain to closely mimic the reference trajectory pattern [14]. The geometry of the task can be approximated from the curvature information of the foot in contact with the ground

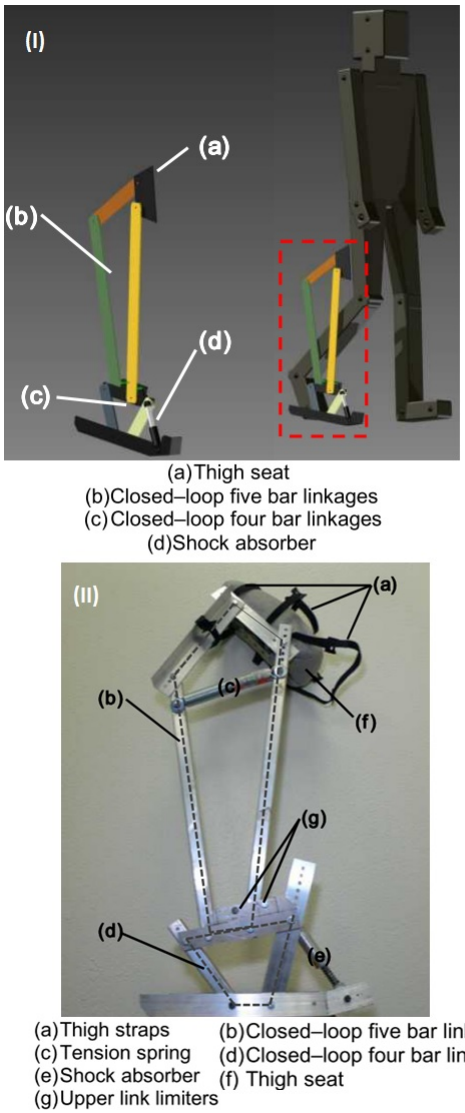

FIGURE 5. The passive crutch substitute TAMC1 with a closed-loop kinematic structure: (I) design of the crutch, (II) prototype of the crutch

in the vicinity of two positions. Figure 8 is an illustration of the general technique. As a next step, the specified contact geometry at the foot is scaled down and transferred to the respective start and end positions at knee level (see Figure 7).

The Synthesis Equations

To design the four bar linkage mechanism for the knee, based on the scaled "tear-drop" trajectory, we first formulate the design equations of a planar RR chain for a contact task. The velocity and acceleration task specifications are derived directly from the scaled curvature information in the start and end positions. The synthesis task is listed in Table 1.

FIGURE 6. Experimental set up: Subject walking on a treadmill, monitored by a 3D Motion Capture System. Reflective markers were attached on the subject's right leg.

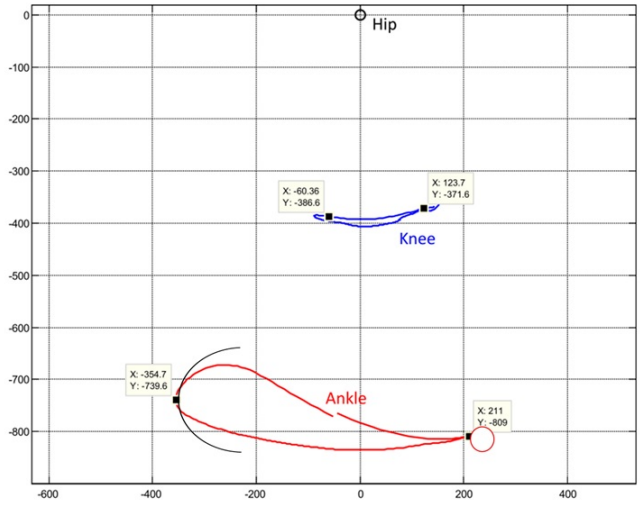

FIGURE 7. Natural walking gait cycle trajectories at foot and knee level, obtained from Vicon Motion Capture System.

TABLE 1. Task data for the synthesis of a planar RR chain.

Posit.	(ϕ, d_x, d_y)	Vel. Data	Accel. Data
1	(0, 2.2, 1.414)	(1, 0.333, 0.934)	(0, 0.290, 0.812)
2	(0, 3.2, 1.5)	(1, -0.0335, -0.8322)	—

The chain has five design parameters the coordinates of the fixed pivot $\mathbf{G} = (u, v, 1)$ in the fixed frame F, the coordinates of the moving pivot $\mathbf{w}$ in the moving frame M, and the length of the crank R. The geometry of the RR chain satisfies the constraint equation:

$$(\mathbf{W} - \mathbf{G}) \cdot (\mathbf{W} - \mathbf{G}) = R^2, \tag{5}$$

where $\mathbf{W}$ defines the fixed frame coordinates of the moving pivot $\mathbf{w}$ as $\mathbf{W}(t) = [T(t)]\mathbf{w}$. Two derivatives of this equation yield the

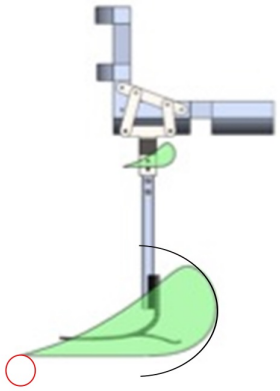

FIGURE 8. General idea of scaling down the task geometry from end-foot to knee level.

additional velocity and acceleration constraint equations

$$\begin{aligned} \dot{\mathbf{W}} \cdot (\mathbf{W} - \mathbf{G}) &= 0, \\ \ddot{\mathbf{W}} \cdot (\mathbf{W} - \mathbf{G}) + \dot{\mathbf{W}} \cdot \dot{\mathbf{W}} &= 0. \end{aligned} \tag{6}$$

The Design Equations

Let $\mathbf{W^1} = (x, y, 1)$, so we have

$$\begin{aligned} \mathbf{W^1}(\mathbf{t}) &= [D^1(t)]\mathbf{W^1} = [I + \Omega^1 t + \frac{1}{2}\Lambda^1 t^2]\mathbf{W^1}, \\ \mathbf{W^2}(\mathbf{t}) &= [D^2(t)]\mathbf{W^2} = [I + \Omega^2 t][D_{12}]\mathbf{W^1}, \end{aligned} \tag{7}$$

where $[D_{12}] = [T_0{}^2][T_0{}^1]^{-1}$ yields $\mathbf{W^2} = [D_{12}]\mathbf{W^1}$.

We substitute the trajectories (7) into the constraint equations (5) and (6) to obtain the design equations for the RR chain.

$$\begin{aligned} \mathscr{P}_1: &\quad 0 = (\mathbf{W^1} - \mathbf{G}) \cdot (\mathbf{W^1} - \mathbf{G}) - R^2, \\ \mathscr{V}_1: &\quad 0 = [\Omega^1]\mathbf{W^1} \cdot (\mathbf{W^1} - \mathbf{G}), \\ \mathscr{A}_1: &\quad 0 = [\Lambda^1]\mathbf{W^1} \cdot (\mathbf{W^1} - \mathbf{G}) + [\Omega^1]\mathbf{W^1} \cdot [\Omega^1]\mathbf{W^1}, \\ \mathscr{P}_2: &\quad 0 = ([D_{12}]\mathbf{W^1} - \mathbf{G}) \cdot ([D_{12}]\mathbf{W^1} - \mathbf{G}) - R^2, \\ \mathscr{V}_2: &\quad 0 = [\Omega^2][D_{12}]\mathbf{W}^1 \cdot ([D_{12}]\mathbf{W^1} - \mathbf{G}). \end{aligned} \tag{8}$$

A detailed algebraic solution procedure of the synthesis incorporating tasks with acceleration specifications could be found in [8]. The synthesis results are shown in Table 2.

The four bar for the passive knee design was constructed by combining the two real solutions, shown in Table 2, resulting in a compact linkage with input and output driving link lengths of $6.17cm$ and $5.06cm$, respectively.

TABLE 2. The two real solutions from the synthesis of the RR chain.

Solution	$\mathbf{G} = (u, v)$	$\mathbf{W} = (x, y)$
1	(2.205, 2.551)	(1.736, 2.150)
2	(0.683, 1.619)	(0.188, 1.510)

Trajectory Planning

The inverse kinematics of the 4R chain yields the joint parameter vector $\mathbf{q}$ at each of the task positions, $i = 1, 2$. In order to obtain the joint velocity vector $\dot{\mathbf{q}}$ at the ith position, we solve the equation

$$V_i = [J_i]\dot{\mathbf{q}}_\mathbf{i}, \quad i = 1, 2, \tag{9}$$

where $V_i = (\omega, \mathbf{v})$ is the velocity prescribed at position i, and J_i is the Jacobian of the 4R chain. Notice that because the Jacobian is a 3×2 matrix, the solution is obtained by pre-multiplying by the inverse of the Jacobian

$$\dot{\mathbf{q}}_{\mathbf{i}i} = [J_i{}^T J_i]^{-1}[J_i{}^T]V_i, \quad i = 1, 2. \tag{10}$$

This is the well-known pseudo-inverse which provides an exact solution because the linkage was designed to satisfy velocity requirement.

Now to determine the joint acceleration vector $\ddot{\mathbf{q}}$, we solve the equation

$$A_i = \dot{J}_i\dot{\mathbf{q}}_i + J_i\ddot{\mathbf{q}}_i, \quad i = 1, \tag{11}$$

where $A_i = (\alpha, \mathbf{a})$ is the acceleration prescribed at the first position and $\dot{J}_i$ is the time derivative of the 3×2 Jacobian matrix. The vector $\dot{J}_i\dot{\mathbf{q}}_i$ is known so we can subtract it from both sides, thus the solution is again obtained using the pseudo-inverse,

$$\ddot{\mathbf{q}}_\mathbf{i} = [J_i{}^T J_i]^{-1}[J_i{}^T](A_i - \dot{J}_i\dot{\mathbf{q}}_i). \tag{12}$$

The trajectory between the joint parameters $(\theta_0, \dot{\theta}_0, \ddot{\theta}_0)$ and $(\theta_f, \dot{\theta}_f, \ddot{\theta}_f)$ over the range $0 \le t \le t_f$ is generated by the fifth degree polynomial

$$\theta(t) = a_0 + a_1 t + a_2 t^2 + a_3 t^3 + a_4 t^4 + a_5 t^5, \tag{13}$$

where

$$\begin{aligned}
a_0 &= \theta_0, \quad a_1 = \dot{\theta}_0, \quad a_2 = \frac{\ddot{\theta}_0}{2}, \\
a_3 &= \frac{20\theta_f - 20\theta_0 - (8\dot{\theta}_f + 12\dot{\theta}_0)t_f - (3\ddot{\theta}_0 - \ddot{\theta}_f)t_f^2}{2t_f^3}, \\
a_4 &= \frac{30\theta_0 - 30\theta_f + (14\dot{\theta}_f + 16\dot{\theta}_0)t_f + (3\ddot{\theta}_0 - 2\ddot{\theta}_f)t_f^2}{2t_f^4}, \\
a_5 &= \frac{12\theta_f - 12\theta_0 - (6\dot{\theta}_f + 6\dot{\theta}_0)t_f - (\ddot{\theta}_0 - \ddot{\theta}_f)t_f^2}{2t_f^5}.
\end{aligned} \tag{14}$$

Equation (13) is obtained by solving the equations defining the joint position, velocity and acceleration evaluated at $t = 0$ and $t = t_f$ to compute the coefficients $a_i, i = 0, \ldots, 5$, see [15]. Figure 9 presents results on the design of the knee which was later incorporated in a passive walking device for people with below knee injury. Figure 9 illustrates the movement of the coupler of the four bar linkage through the task, shown in Table 1. The coupler maintains contact with a virtual object shown by the circle in the first location, due to the task acceleration, which implies contact curvature specification. In the second position, the coupler is in contact with another objects, due to the specified task velocity.

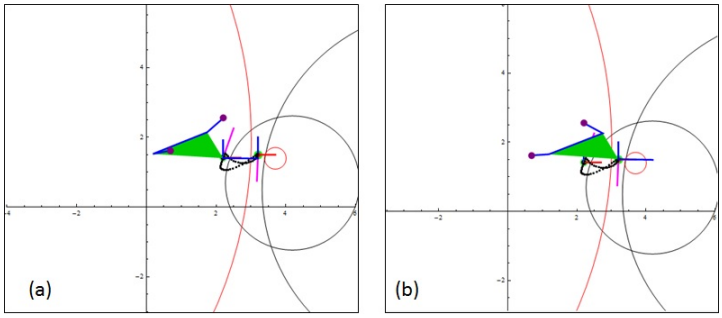

FIGURE 9. The four bar linkage synthesized for the knee design of the passive assistive walking device for a lower leg injury. The four bar linkage is self-locking in the first and second positions. The figure also shows the obtained scaled down "tear drop" shape trajectory.

Note that due to the task acceleration defined in the first position the designed chain follows closely the desired trajectory in the vicinity of that position.

Figure 10 and Figure 11 present the passive walking device with the four-bar knee incorporated.

Performance of the Device

The design of the crutch substitute was completed using statistical averages of anthropometric data. By determining the av-

FIGURE 10. The passive walking device, incorporating two four bar linkages on both sides of the knee. The four bar linkage at the knee follow a scaled down "tear-drop trajectory", obtained from actual human walking trajectory at foot level.

FIGURE 11. Prototype of the passive walker.

erage leg sizes of possible users, a design was created to fit people of different sizes by providing adjustable strapping. The end result was a form-fitting, comfortable, and adjustabe crutch substitute that is strong, sturdy, and lightweight. In order to feel natural and comfortable, the device had to provide enough stability for the user to control. Several features of the passive walker increase the stability of the device. The four-bar linkage knee design allows for a more stable range of motion than a hinge joint knee design due to a large range of motion where the instant center of the four-bar linkage lies within a stability region. For stability, the ICR needs to be in front of the action line of GRF in the first position, between the GR lines in stance and behind the GRF line in the second position [1]. Due to the fact that the instant center of rotation (ICR) of the four-bar is variable, it plays a major role into defining the system stability, which is achieved through the knee mechanism and the ground reaction force (GRF), shown in Figure 11 and Figure 12.

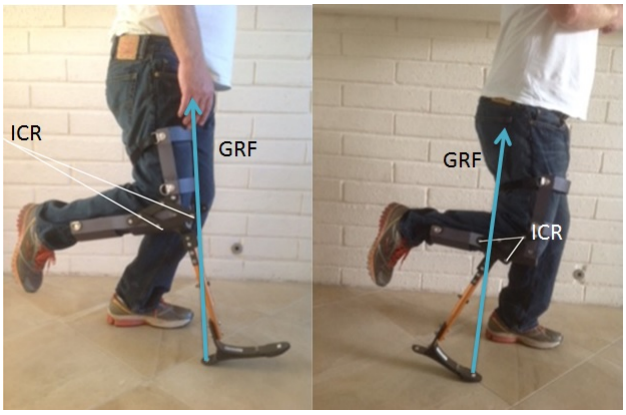

FIGURE 12. The stability of the passive knee joint can be examined by the position of the Instantaneous Centre of Rotation with respect to Ground Reaction Force.

The form-fitting design of the leg attachment also provides enhancements to stability. The design fits securely to the user's leg and the foot extension touches the ground where the users own foot would be expected to be. This natural location allows the user to quickly respond to slight deviations in ground level and provides for a smaller learning curve. Since the stability of the device will also depend on the dexterity of the user, a smaller learning curve will make for a more stable device. Lastly, the toes of a human foot assist in providing stability. They essentially "grab" the floor and provide a stable platform when ground surfacing is uneven. In relation to that, the prosthetic foot chosen for this project contains a split-toe feature providing lateral stability. The manufacturability of the crutch was improved to lower production times and weight-bearing components were adjusted to increase the strength and fatigue life of the device.

For validation, the passive walker was tested to determine if the design requirements and project goals are met. Dynamic testing was performed at the Human Interactive Robotics laboratory with the assistance of the Kinesiology department at California State University, Fullerton. Users initially walked on a treadmill without the device to determine the trajectories of three key body points: the hip, knee, and ankle. The users then walked with the device attached. The trajectories of the key points with the device attached were then compared to the trajectories of the key points without the device. The result from the motion profile of walking on the treadmill with the device showed that the device is not able to mimic well the natural shape throughout the profile successfully. However, it is necessary to emphasize that walking on the treadmill is very different from walking on the ground. The foot, which is made of rubber, sticks easily on the treadmill and so it is harder to walk. Thus, a second series of experiments

were performed, where a number of subjects were walking on the floor with the device attached. The comparison between the natural walking trajectory and the averaged results of the subjects walking with the device showed that the device is able to achieve close to 75% of the natural gait.

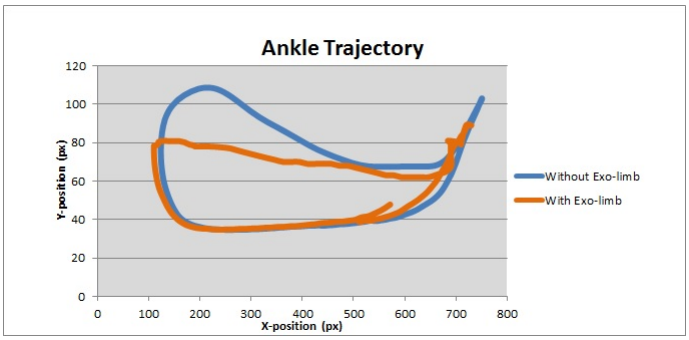

FIGURE 13. Motion profile of the passive crutch device while walking on ground.

SUMMARY

The focus of this research has been on creating a passive lower extremity wearable device that mimics humans natural walking gait incorporating a four bar linkage knee. The knee design is based on anthropomorphic foot walking trajectory obtained from optical motion capture system. The task geometry at the foot, related to contact and curvature constraints of the foot with the ground at two critical positions heel strike and toe off, is scaled to the knee level and then velocity and acceleration specifications compatible with the task geometry at the knee joint are derived. These higher order motion constraints assist in defining the synthesis equations for the knee design. A working prototype of a passive crutch substitute for people with below knee injuries incorporating the mechanical knee shows the applicability of the proposed technique. The research and developments made in this paper with regard to designing compact mechanical devices, able to mimic natural limb motion are important contributions that find future applications in areas such as robotic locomotion and grasping.

ACKNOWLEDGMENT

The authors gratefully acknowledge the assistance of Mr. Jason Taylor, Senior Project Manager at Ossur America, the Exo-Limb team at California State University, as well as the support of NSF Grant, Award Id: IIS-1208412, sub-award Id: 2013-2908, and NSF Grant, Award 140411.

REFERENCES

[1] Xie, H.-L., Liang, Z.-Z., Li, F., and Guo, L.-X., 2010. "The knee joint design and control of above-knee intelligent bionic leg based on magneto-rheological damper". *International Journal of Automation and Computing,* ***7***(3), pp. 277–282.

[2] Parenti-Castelli, V., Leardini, A., Di Gregorio, R., and O'Connor, J. J., 2004. "On the modeling of passive motion of the human knee joint by means of equivalent planar and spatial parallel mechanisms". *Autonomous Robots,* ***16***(2), pp. 219–232.

[3] Radcliffe, C., 1994. "Four-bar linkage prosthetic knee mechanisms: kinematics, alignment and prescription criteria". *Prosthetics and orthotics international,* ***18***(3), pp. 159–173.

[4] De Vries, J., 1995. "Conventional 4-bar linkage knee mechanisms: a strength-weakness analysis.". *Journal of rehabilitation research and development,* ***32***(1), pp. 36–42.

[5] Sancisi, N., Caminati, R., and Parenti-Castelli, V., 2009. "Optimal four-bar linkage for the stability and the motion of the human knee prostheses". In Atti del XIX CONGRESSO dell'Associazione Italiana di Meccanica Teorica e Applicata. Ancona, pp. 1–10.

[6] Hamon, A., and Aoustin, Y., 2010. "Cross four-bar linkage for the knees of a planar bipedal robot". In Humanoid Robots (Humanoids), 2010 10th IEEE-RAS International Conference on, IEEE, pp. 379–384.

[7] Jin, D., Zhang, R., Dimo, H., Wang, R., and Zhang, J., 2003. "Kinematic and dynamic performance of prosthetic knee joint using six-bar mechanism". *Journal of rehabilitation research and development,* ***40***(1), pp. 39–48.

[8] Robson, N. P., and McCarthy, J. M., 2007. "Kinematic synthesis with contact direction and curvature constraints on the workpiece". In ASME 2007 International Design Engineering Technical Conferences and Computers and Information in Engineering Conference, American Society of Mechanical Engineers, pp. 581–588.

[9] Tesar, D., and Sparks, J., 1968. "The generalized concept of five multiply separated positions in coplanar motion". *Journal of Mechanisms,* ***3***(1), pp. 25–33.

[10] Dowler, H., Duffy, J., and Tesar, D., 1978. "A generalised study of four and five multiply separated positions in spherical kinematicsii". *Mechanism and Machine Theory,* ***13***(4), pp. 409–435.

[11] Rimon, E., and Burdick, J. W., 1995. "A configuration space analysis of bodies in contacti. 1st order mobility". *Mechanism and Machine Theory,* ***30***(6), pp. 897–912.

[12] Rimon, E., and Burdick, J. W., 1995. "A configuration space analysis of bodies in contactii. 2nd order mobility". *Mechanism and machine theory,* ***30***(6), pp. 913–928.

[13] Robson, N. P., and McCarthy, J. M., 2005. "The synthesis of planar 4r linkages with three task positions and two

specified velocities". In ASME 2005 International Design Engineering Technical Conferences and Computers and Information in Engineering Conference, American Society of Mechanical Engineers, pp. 425–432.

[14] Moon, H., Baumgartner, H., and Robson, N. P., 2011. "Toward a 21 st century crutch design for assisting natural gait".

[15] Craig, J. J., 2005. *Introduction to robotics: mechanics and control*, Vol. 3. Pearson Prentice Hall Upper Saddle River.